

Exploring biological influence on offshore sandwave length

B.W. Borsje

Department of Water Engineering and Management, University of Twente, Enschede, The Netherlands
WL/Delft Hydraulics, Marine and Coastal Systems, Delft, The Netherlands

G. Besio

Department of Civil, Environmental and Architectural Engineering, University of Genoa, Genoa, Italy

S.J.M.H. Hulscher

Department of Water Engineering and Management, University of Twente, Enschede, The Netherlands

P. Blondeaux & G. Vittori

Department of Civil, Environmental and Architectural Engineering, University of Genoa, Genoa, Italy

ABSTRACT: Biological activity at the seabed is known to have a significant influence on bottom dynamics and morphology. This paper explores the influence of biological activity on sand wave dimensions by adapting the input parameters of an idealized sandwave model (Besio et al., 2006). Once the prediction capability of the model is analyzed by means of a comparison of the theoretical predictions with different field data in the Belgium Continental Shelf, the values of the physical parameters are changed (the critical bed shear stress is lowered because of the burrowing activity of surface deposit feeders and the ripple height is lowered because of tube building worms) and the trends of the wavelength as function of the parameters are analyzed. The results show that the predicted wavelengths are closer to the observed values if biological activity is included in the model. Once the significant influence of biological activity on sandwave dimensions is shown, future research should focus on a better parameterization of biological activity in order to improve the reliability of the long-term morphodynamic predictions, especially in marine environments with large biological activities.

1 INTRODUCTION

On the bed of the North Sea, sand waves are often present, which grow up to 25% of the water depth and migrate at a speed of tens of metres per year (Németh et al., 2002, Besio et al., 2004). These sand waves can pose a hazard to offshore constructions, navigation channels, pipelines and telecommunication cables. On the other hand, bed forms can protect the coastline against storms.

The bottom of the North Sea is also covered by a great number of organisms which live in and on the bottom (Heip et al., 1992; Künitzer et al., 1992; Rabaut et al., 2007). These benthic organisms try to optimize their habitat, resulting in biogeomorphological interactions.

Given both the strong seasonal and spatial variation of the biomass benthic organisms in temperate subtidal regions (Knaapen et al., 2003; Van Hoey et al., 2004; Baptist et al., 2006), a strong variation in the abiotic parameters should be expected.

The precise interaction between the biological activity and morphodynamics is not known at this moment. Such knowledge is of great interest for reliable long-term morphodynamic predictions, especially in marine environments with large biological activity.

The aim of this paper is to explore the influence of biological activity on the sand wave size. Hereto, an idealized model (Besio et al., 2006) is used which was proven to fairly predict sand wave dimensions for both the Belgium and French Continental Shelves (Cherlet et al., 2007). In particular, we look at two different types of biological influences: destabilizing and stabilizing effects on the stability of the bed by biota. These effects are mimicked by decreasing the critical bed shear stress and by decreasing the ripple height used in the simulations respectively. As a result, a first insight can be obtained in the possible biological influence on the sandwave dimensions.

The structure of the paper is as follows. Section 2 introduces the study area. Next, in Section 3, we present the idealized model. Section 4 discusses the outcomes of the model as the physical input parameters are varied and compares the theoretical predictions with field observations. In Section 5 the biological processes are included in the model and the improved agreement of the predictions with field observations is shown. Section 6 presents a discussion about the main findings of the paper. We end by drawing some conclusions in the final section.

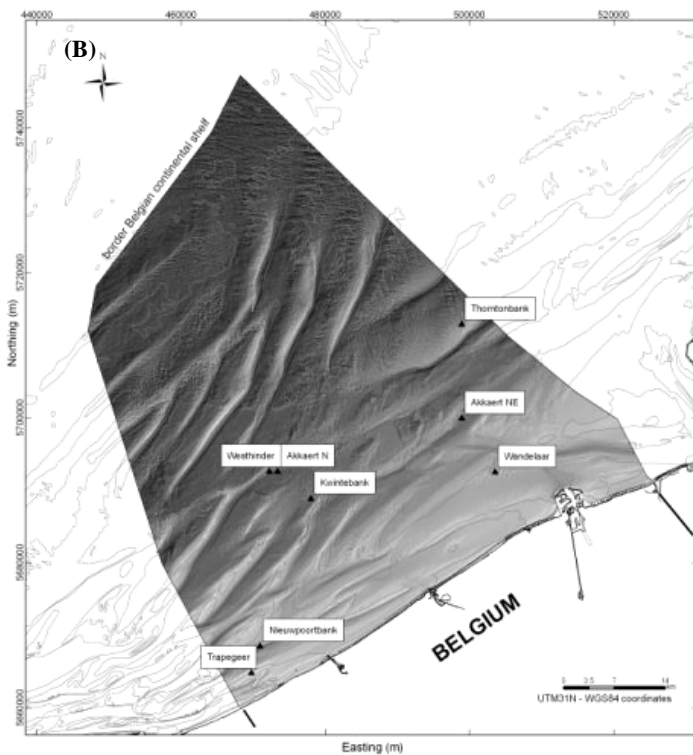
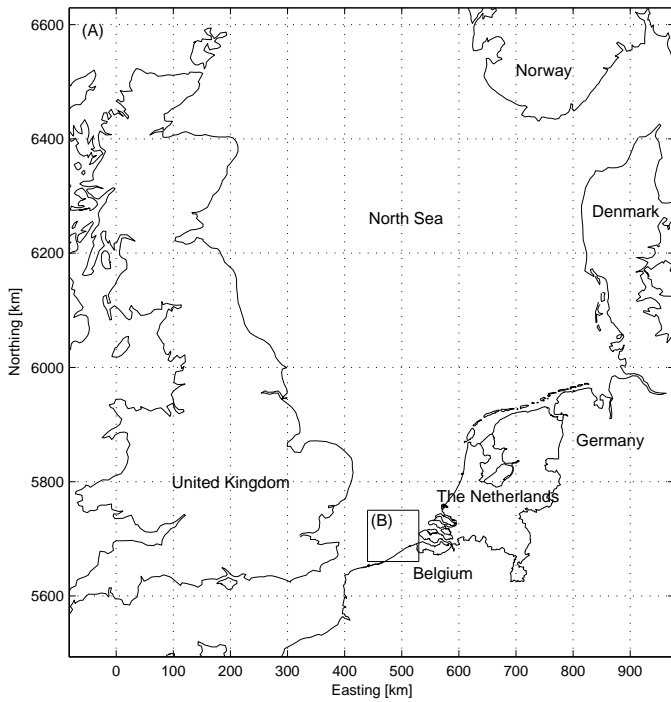


Figure 1. Seabed patterns in the Belgium Continental Shelf (B), located in the Southern North Sea (A). Field sites included for later reference (adapted from Cherlet et al., 2007).

2 STUDY AREA

The study area is situated in the southern part of the North Sea (Figure 1) and covers the Belgium Continental Shelf (2600 km²). Several sand bank systems are located in this shallow area, where the water depths are smaller than 35 m. Tides are predominantly semi-diurnal, with maximum flow velocities ranging between 0.50 and 0.70 m s⁻¹.

Table 1. Habitat preferences of the four macrobenthic communities at the Belgium Continental Shelf. Mean values for the average grain size (D_{50}), slope (S), mud content (M_c), distance offshore (D_{off}) and water depth (H), based on 690 samples.

	D_{50} [mm]	S [%]	M_c [%]	D_{off} [km]	H [m]
<i>Macoma balthica</i>	0.08	0.15	50	3	7
<i>Abra alba</i>	0.22	0.38	10	8	13
<i>Nephtys cirrosa</i>	0.28	0.50	0	22	13
<i>Ophelia limacina</i>	0.42	0.55	0	40	30

The soft sediment macrobenthic community structure on the Belgium Continental Shelf is described by Degraer et al. (2003) and Van Hoey et al. (2004) and comprises four subtidal communities: (1) *Macoma balthica* (baltic telling), (2) *Abra alba* (white furrow shell), (3) *Nephtys cirrosa* (white worm) and (4) *Ophelia limacina* (bristle worm). Table 1 summarizes the clear differences in habitat preferences for these macrobenthic communities (Degraer et al., in press).

3 THEORETICAL MODEL

As pointed out by Hulscher (1996), Gerkema (2000) and Besio et al. (2006), the process which leads to the formation of sand waves is similar to that originating sea ripples under gravity waves (Sleath, 1984; Blondeaux, 1990; Blondeaux, 2001). The interaction of the oscillatory tidal flow with bottom perturbations gives rise to a steady streaming in the form of recirculating cells. When the net displacement of the sediment dragged by this steady streaming is directed toward the crests of the bottom waviness, the amplitude of the perturbation grows and bedforms are generated. On the other hand, the flat bottom configuration turns out to be stable when the net motion of the sediment is directed toward the troughs of the bottom waviness.

The theoretical investigation of sand wave appearance forced by tide propagation has been mainly carried out by means of linear stability analyses (Hulscher, 1996; Gerkema, 2000; Komarova & Hulscher, 2000; Besio et al., 2003; Besio et al., 2006) which study the initial development of arbitrary bottom perturbations of small amplitude superimposed to the flat bottom configuration. Random initial perturbations contain different spatial components which are characterized by dimensionless wavenumbers α_x , α_y in the horizontal directions x and y and, in the linear approximation, evolve each independently of the other. Hence, a normal-mode analysis can be applied and the generic component of the perturbation can be considered. The time development of the perturbation of the sea bottom is controlled by the sediment balance which leads to Exner equation. To integrate such an equation, a predictor for the sediment transport rate is needed and the flow field must be evaluated. Different models can be used to solve the hydrodynamic problem, to evaluate the

bottom shear stress and to quantify the sediment transport. However, the solution procedure invariably leads to an amplitude equation for the bottom perturbation in the form

$$\frac{dA(t)}{dt} = \Gamma(t) A(t) \quad (1)$$

where $A(t)$ is the amplitude of the perturbation and the complex function $\Gamma(t) = \Gamma_r(t) + i\Gamma_i(t)$ depends on suitable flow and sediment parameters. Since the forcing tidal flow is time periodic, the quantity $\Gamma(t)$ turns out to be a periodic function and the growth of the bottom forms is controlled by the time average $\bar{\Gamma}$ of Γ . A linear stability analysis suggests that the component of the bottom perturbation characterized by the largest value of the amplification rate (amplification rate = time averaged value of $\Gamma(t)$) will prevail for large times. Hence, a linear analysis predicts a specific wavelength, an orientation and a migration speed of the most unstable component of the bed perturbation which can be assumed to coincide with the appearing bedforms (for more details on the theoretical approach, the interested reader is referred to Dodd et al., 2003).

To develop the hydro- and morpho-dynamic models, it is convenient to consider the dimensionless problem, where the mean water depth h_0^* is used as length scale, the maximum value U_0^* of the depth averaged fluid velocity during the tidal cycle is used as velocity scale and the inverse of the angular frequency of the tide ω^* is used as timescale. The dimensionless hydrodynamic problem is characterized by two main dimensionless parameters, beside the values of $\Omega = \Omega^*/\omega^*$ (rate of earth rotation) and ϕ_0 (latitude), which control the velocity profile:

$$k_c = \frac{U_0^*}{\omega^* h_0^*} \quad \hat{\mu} = \frac{C}{\kappa \int_{-1}^0 F(\xi) d\xi} \quad (2a,b)$$

where C is a friction coefficient evaluated by means of standard formulas for steady currents (see a.o. Fredsoe & Deigaard, 1992) employing the roughness due to the presence of ripples. Moreover, the function $F(\xi)$ ($\xi = z^*/h_0^*$) describes the vertical structure of the eddy viscosity and it has been chosen as suggested by Dean (1974).

The time development of the bottom configuration is provided by the sediment continuity equation along with a sediment transport predictor. The dimensionless parameters which characterize the morphodynamic problem are the sediment porosity p_{or} , the dimensionless sediment size d , the mobility number Ψ_d and the Reynolds number R_p of sediment particles defined as follow:

$$d = \frac{d^*}{h_0^*} \quad \Psi_d = \frac{(\omega^* h_0^*)^2}{(\rho_s^*/\rho^* - 1) g^* d^*} \quad (3a,b)$$

$$R_p = \frac{\sqrt{(\rho_s^*/\rho^* - 1) g^* d^*}}{v^*} \quad (4)$$

Important parameters in the bio-geomorphological interactions (Section 5) are the dimensionless bed load transport (q_{Bx}, q_{By}) induced by the tidal current (5) and the dimensionless height of the ripples (Δ_r) (6) which are both dependent on the Reynolds number of the sediment particles.

$$\begin{aligned} (q_{Bx}, q_{By}) &= \frac{(q_{Bx}^*, q_{By}^*)}{\sqrt{(\rho_s^*/\rho^* - 1) g^* d^{*3}}} = \\ &= \frac{0.25}{R_p^{0.2}} \left(\frac{\theta - \theta_{cr}}{\theta_{cr}} \right)^{1.5} \left(\frac{\theta_x, \theta_y}{\sqrt{\theta}} \right) \end{aligned} \quad (5)$$

$$\Delta_r = 202 d R_p^{-0.369} \quad (6)$$

The θ_x and θ_y are the x - and y - components of the Shields parameter θ and θ_{cr} is its critical value below which no sediment moves. Of course (q_{Bx}, q_{By}) vanishes when θ is smaller than θ_{cr} . In (6) ripple height is computed according to Soulsby & Whitehouse (2005). Moreover, following the suggestion of Van Rijn (1991), the roughness height z_r is fixed equal to Δ_r .

Previous studies (Hulscher & Van den Brink, 2001; Van der Veen et al., 2006) investigated the capability of stability analyses to predict the occurrence of sand waves. However, the above works did not attempt to predict the geometrical characteristics of the bottom forms.

4 FIELD OBSERVATIONS AND TRENDS

Sand wave dimensions along the Belgium Continental Shelf were modeled by Cherlet et al. (2007) for 7 different sites, based on site specific information on the water depth h_0^* , flow velocity U_0^* and grain size d^* (Figure 1b). The sensitivity of the model results for a variation of h_0^* , U_0^* and d^* is shown in Figure 2a-c. The variation of the wavelength is plotted by varying one of the input parameters while keeping constant the others and equal to the values measured in the field. The field measurements of the wavelength are included in the plots too.

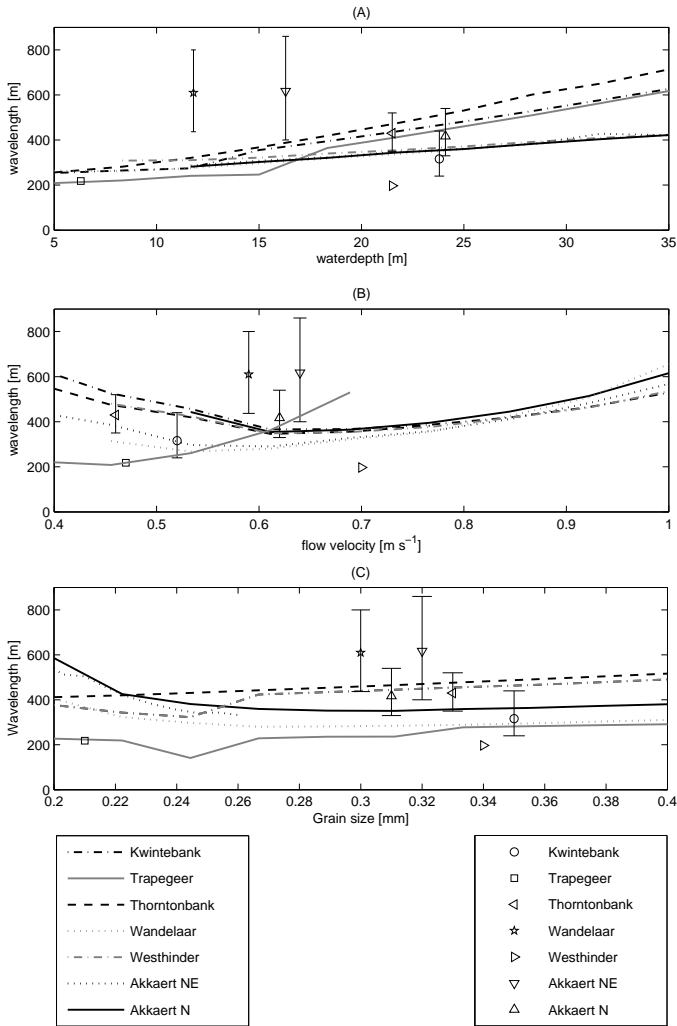


Figure 2. Wave length of the sandwaves obtained by varying waterdepth (a), flow velocity (b) and grain size (c) for different sites on the Belgium Continental Shelf. Model results are described by lines, field measurements are described by markers.

By increasing the water depth (Figure 2a), the wavelength of the sand waves increases almost linearly. This observation is the result of a linear decrease in the Shields parameter for an increase of waterdepth (Besio et al., 2007), resulting in longer sandwaves.

By increasing the flow velocity (Figure 2b), first the Shields parameter θ becomes larger than the critical Shield parameter which gives rise to sandwaves (see for example the Wandelaar site). A further increase of the flow velocity leads to larger values of the growth rate and the flat bottom configuration turns out to be more unstable. Moreover the value of α_x , which characterizes the most unstable mode, increases thus showing that stronger tidal currents tend to generate shorter sand waves. However, the wavelength of the sandwaves shows a minimum. Indeed for very strong tidal currents, the suspended sediment starts to become relevant and to provide a significant stabilizing contribution to the phenomenon, resulting in longer sandwaves. Eventually, the contribution of the suspended sediment is so large that the flat bed turns out to be stable.

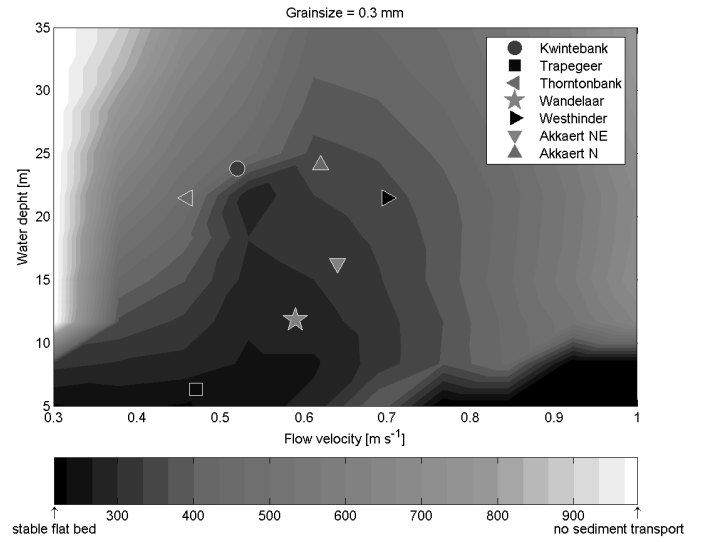


Figure 3. Comparison between the predicted wavelengths (surface area) and the field measurements (filled markers) [m]. The predicted wavelengths are obtained as function of the flow velocity and waterdepth while keeping constant the grain size (0.3 mm). Black areas indicate a stable flat bed, while the white areas indicate when no sediment transport is induced by the tidal current.

For small grain sizes (Figure 2c), the suspended load provides a significant contribution to the growth rate of the bottom perturbations. However, if the grain size is increased, the contribution of the suspended load to the growth of the bottom forms decreases and eventually vanishes and the net growth rate of the bottom perturbations is controlled by a balance between the destabilizing effect due to the bed load and the stabilizing one due to the bottom slope, resulting in an almost constant wavelength of the bottom forms.

At four sites, the predicted sand wave dimensions agree well with field measurements (Figure 2). However, at Akkaert NE, Wandelaar and Westhinder sites, the predicted wavelength slightly deviates from the field measurements.

Since the grain size is almost the same ($d \sim 0.3\text{mm}$) at the different sites, it is valuable to compare the model results and field measurements by varying flow velocity and waterdepth (Figure 3), while keeping fixed the value of the diameter.

Figure 3 indicates that for the three sites in which the measured wavelengths differ from the measurements, the result do not improve by varying the waterdepth or the flow velocity.

Table 2. Spatial distribution of the surface deposit feeder *Macoma balthica* and the tube building *Lanice conchilega* for the different sites located on the Belgium Continental Shelf.

	<i>Macoma balthica</i>	<i>Lanice conchilega</i>
Kwintebank		x
Trapegeer	x	
Thorntonbank	x	
Wandelaar	x	
Westhinder		x
Akkaert NE	x	
Akkaert N		x

5 MODELING BIOLOGICAL INFLUENCES

As shown in Table 2, different biota are present in the considered sites on the Belgium Continental Shelf (Rabaut et al, 2007; Degreuer et al., in press).

The presence of biota influences the stability of the bed in two opposite ways. *Macoma balthica* is well-known for its destabilising effect on the bed, because of its burrowing and feeding activities (e.g. Austen et al., 1999). In the Western Wadden Sea, *Macoma balthica* is responsible for a reduction of the critical bed shear stress up to a factor 0.5, resulting in a significant influence on the fine sediment distribution on the bed (Borsje et al., 2007).

In *Lanice conchilega* assemblages, the velocity of the near-bottom flow is reduced and the normal, laminar near-bottom flow is deflected around and across the assemblages (Eckman, 1983). Flow velocity plays an important role in the formation and geometry of the ripples, as shown by O'Donoghue et al. (2006) who performed flume experiments in full-scale oscillatory flows. As a result, *Lanice conchilega* influences the height of the ripples which are present on the top of the sand waves and are the main origin of the bottom roughness.

A well accepted parameterization of the influence of *Macoma balthica* and *Lanice conchilega* on the stability of the subtidal bed is not available, therefore assumptions are made on the biological adjustments of the model parameters. The influence of biological activity on the critical value of the Shields parameter and roughness height is quantified by:

$$\theta_{cr} = \theta_{cr}^d T_d (\text{Macoma}) \quad (7)$$

$$z_r = z_r^d E_s (\text{Lanice}) \quad (8)$$

where T_d and E_s are the (de)stabilizing biological factors for the critical bed shear stress for erosion and ripple height respectively (see equation 5 and 6). The superscript 'd' for the critical shear stress and ripple height represents the values without the influence of biological activity (default). The destabilizing biological factors are dependent on the density of *Macoma balthica* and *Lanice conchilega*.

The biomass *Macoma balthica* in the subtidal area is almost a factor five smaller compared to the intertidal area (Heip et al., 1992). Therefore, following the parameterization given by Borsje et al. (2007) for intertidal areas, the critical bed shear stress is reduced by a factor 0.65 due to the burrowing activity of *Macoma balthica*.

Eckman et al. (1981) found a reduction of the flow velocity within a cluster of tubes up to a factor 0.5 due to the presence of tube building animals. Following the ripple dimensions given by O'Donoghue et al. (2006), this reduction will result in a decrease of the ripple height by a factor 0.6 due

to the deceleration of the near-bottom flow by *Lanice conchilega*.

By including both the stabilizing and destabilizing effects of biota in the model ($T_d = 0.65$; $E_s = 0.6$), the predicted wavelength of the sandwaves at the different sites changes. The relative changes due to both the decrease of critical bed shear stress and the lowering of the ripple height are shown in Figure 4a and 4b respectively. The absolute wavelength for the case in which *Macoma balthica* and *Lanice conchilega* are included is shown in Figure 4c and 4e respectively.

Due to the presence of *Macoma balthica*, the sediment is more prone to erosion and therefore the amount of sediment in suspension is larger compared to the case in which no biological activity is included. The higher suspended sediment concentration results in a stable flat bed for large flow velocities (Figure 4c). Moreover, the area of no sediment transport is decreased relative to the default case, due to the burrowing activity of *Macoma balthica*. Finally, the minimum in the wavelength and flow velocity relation as found in Figure 2b, is located at a smaller flow velocity, while the suspended sediment contribution for equal flow velocities is larger for the simulation in which *Macoma balthica* is included.

The presence of *Lanice conchilega* results in a smaller roughness height and therefore a lower eddy viscosity, since the eddy viscosity is assumed to be proportional to the time average of the local friction velocity and to the local depth (Besio et al., 2006). As a result, the local suspended sediment concentrations are lower than the default case.

The difference in wavelengths due to *Lanice conchilega* for low flow velocities (Figure 4b) is very small, due to the small height of the ripples and corresponding low suspended sediment contribution to the total transport in both cases. Moreover, the Shields parameter decreases due to the lowering of the roughness height, resulting in higher bed load transport compared to suspended load. As a consequence, the wavelength for large water depths are much smaller, compared to the case in which no biological activity is included.

While the biological activity influences the sediment dynamics and hydrodynamics in multiple ways, the change in wavelength is not easy to predict, as can be seen in Figure 5a and 5b, where the general trend shows an increase of wavelength due to the burrowing effect of *Macoma balthica* and a decrease of wavelength due to the reduction of the near-bottom velocity by *Lanice conchilega*. For the sites in which the wavelength agrees well with the field measurements using the default model, the biological activity predicts almost the same wavelength (Trappegeer and Thorntonbank)

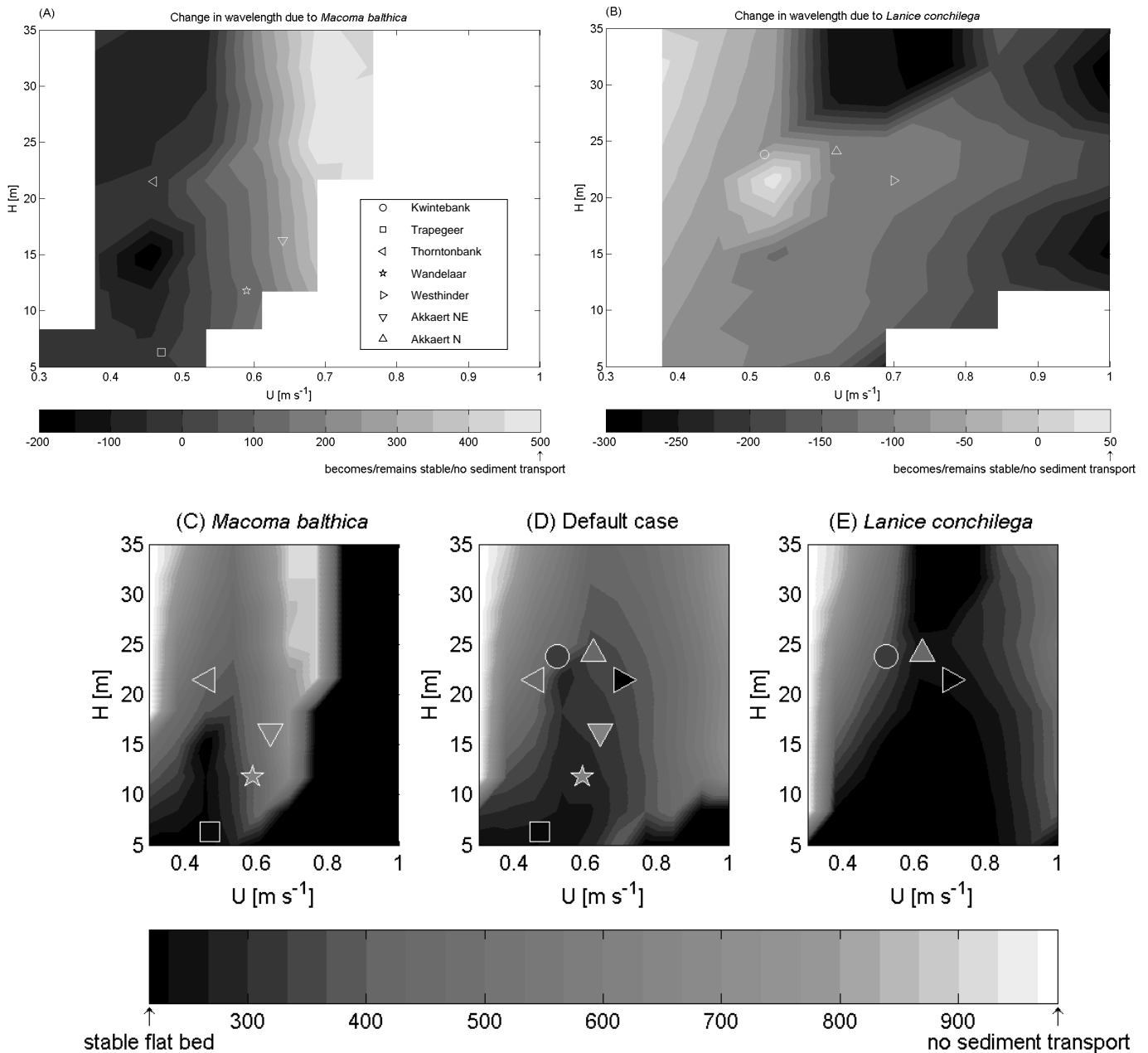


Figure 4. Relative change in the modeled wavelength [m] due to the lowering of the critical bed shear stress by *Macoma balthica*: $T_d = 0.65$ (a), and the decrease of the ripple height by *Lanice conchilega*: $E_s = 0.6$ (b), based on the difference in wavelength shown in (c-e). Positive values indicate an increase in wavelength relative to the physical model. Markers are included based on the present biota (Table 2) and filled with the corresponding colors from field measurements. White areas in (a-b) indicate a transition from stable/no sediment transport to sandwaves and vice versa, or no change in sediment transport/stable flat bed. Note the difference in color limits for the different figures.

6 DISCUSSION

This paper explores the influence that biota have on the wavelength of sand waves on the Belgium Continental Shelf.

The comparisons between the predicted wavelengths and the measurements for both the morphological approach (Cherlet et al., 2007) and the bio-morphological one are shown in Figure 6.

In this exploration, we only took in account two species. However, the biodiversity in the study area is much larger. Moreover in other regions, other

biogeomorphological interactions need to be included. Finally, the biomass of the different species is not constant in time and place as already pointed out in the introduction. As a result, to improve the geomorphological predictions, more accurate parameterizations of the bio-geo-morphological interactions need to be proposed for the different biota, which can be based on the formulations given in equation 7 and 8.

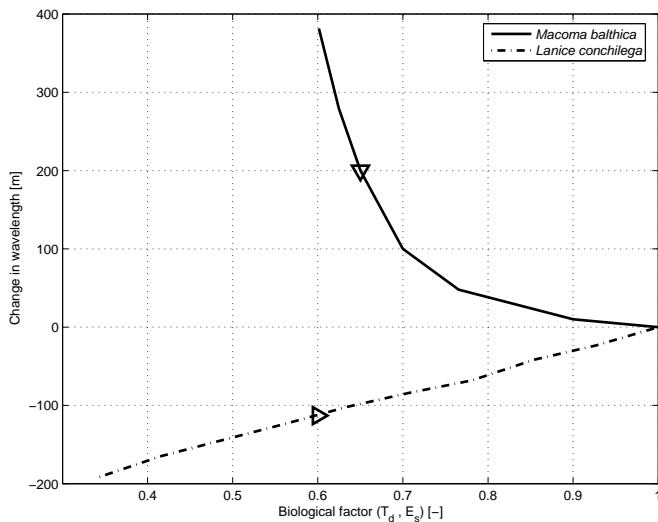


Figure 5. Changes of the wavelength as function of variation in the biological factor for the sites Akkaert NE and Westhinder. The biological factor (T_d and E_s) is defined in equation 7 and 8. Markers show the setting of the biological factor used in this study.

The decrease in the predicted wavelength at the sites where *Macoma balthica* is present and the increase in the predicted wavelength at the sites where *Lanice conchilega* is active are in agreement with the field measurements (Figure 6).

However, the modification of the input parameters is not completely known. Therefore, Figure 5 shows the variation of the predicted wavelength for the Akkaert NE and Westhinder sites based on a variation in the biological factor T_d and E_d .

The influence of *Macoma balthica* on the sandwave dynamics is larger than that due to *Lanice conchilega* despite the large biological factor associated to the latter macrobenthic community.

The model used in this study is based on a linear stability analysis, hence the biological influence on the height of the sandwaves can not be predicted. Moreover, the biological influence on migration rate of sandwaves is not investigated in this study. Therefore, including biological activity in a non-linear model is recommended as well as the formulation of the model which takes into account the presence of residual current and interaction of different tide constituents.

All predicted wavelengths obtained including biological activity show an improved agreement with field measurements except for the Akkaert N site. At this site, the physical parameters are almost the same as for the Westhinder site (Figure 3), suggesting that the wavelength is not only dependent on physical processes. By including biological activity in the model, the Westhinder prediction improves, while the Akkaert N prediction is better in the physical model. This observation suggests that at the Akkaert N site the biomass *Lanice conchilega* is smaller compared to the Westhinder site.

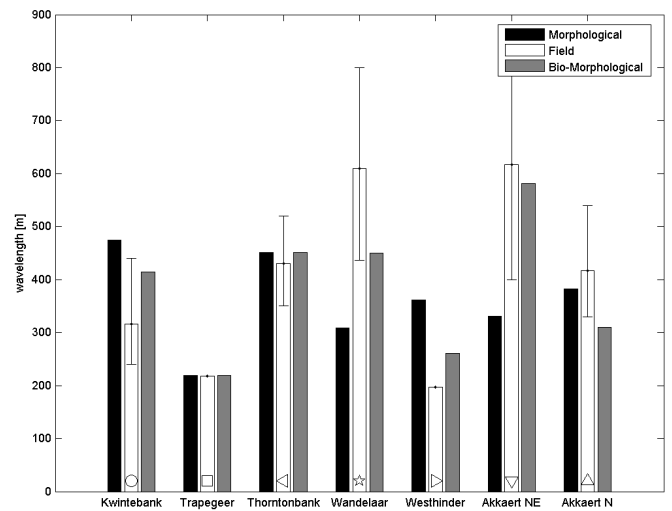


Figure 6. Comparison between the predicted and measured wavelength of the sandwaves at the different sites for both the morphological model (Cherlet et al., 2007) and the bio-morphological model. Markers at the bottom of the plot correspond to the markers used in Figure 4.

7 CONCLUSIONS

This study demonstrates the influence of biological activity on the length of sandwaves. Moreover, it shows that the inclusion of biological activity in an idealized model leads to a better agreement between the modeled sandwave length and the field measurements.

Biological activity is shown to have different effects on sandwave dimension. In general, the burrowing activity by *Macoma balthica* results in an increase of the predicted wavelength, while the tube building *Lanice conchilega* reduces the predicted wavelength of sandwaves, since it reduces the ripple height on top of the large scale bottom forms. However, opposite influence on sandwave length changes is also possible due to diverse influence on both the sediment dynamics and hydrodynamics by the biota.

The results show the importance of incorporating biological activity in morphodynamic models to help to formulate recommendations for the management and conservation of shallow tidal seas characterized by large biological activities.

REFERENCES

- Austen, I., Andersen, T.J. & Edelvang, K., 1999. The influence of benthic diatoms and invertebrates on the erodibility of an intertidal mudflat, the Danish Wadden Sea. *Estuarine, Coastal and Shelf Science* 49, 99-111.
- Baptist, M.J., van Dalen, J., Weber, A., Passchier, S. & van Heteren, S., 2006. The distribution of macrozoobenthos in the Southern North Sea in relation to meso-scale bedforms. *Estuarine, Coastal and Shelf Science* 68, 538-546.

- Besio G., Blondeaux, P. & Frisina, P. 2003. A note on tidally generated sand waves. *Journal of Fluid Mechanics* 485, 171-190.
- Besio G., Blondeaux, P., Brocchini, M. & Vittori, G. 2004. On the modelling of sand wave migration. *Journal of Geophysical Research* 109, C04018, doi:10.1029/2002JC001622.
- Besio, G., Blondeaux, P. & Vittori, G., 2006. On the formation of sand waves and sand banks. *Journal of Fluid Mechanics* 557, 1-27.
- Blondeaux, P., 1990. Sand ripples under sea waves: Part I. Ripple formation. *Journal of Fluid Mechanics* 218, 1-17.
- Blondeaux, P., 2001. Mechanics of coastal forms. *Annual Review of Fluid Mechanics* 33, 339-370.
- Borsje, B.W., Hulscher, S.J.M.H., De Vries, M.B. & De Boer, G.J., 2007. Modeling large scale cohesive sediment transport by including biological activity. Eds. Dohmen-Janssen and Hulscher, *Proceedings fifth IAHR Symposium on River, Coastal and Estuarine Morphodynamics*, 255-262.
- Cherlet, J., Besio, G., Blondeaux, P. van Lancker, V., Verfaillie, E. & Vittori, G., 2007. Modeling sand wave characteristics on the Belgian Continental Shelf and in the Calais-Dover Strait. *Journal of Geophysical Research*, Vol. 112, C06002, doi:10.1029/2007/JC004089.
- Dagraer, S., Verfaillie, E., Willems, W., Adriaens, E., Vincx, M. & Van Lancker, V., in press. Habitat suitability modelling as a mapping tool for macrobenthic communities: An example from the Belgian part of the North Sea. *Continental Shelf Research*.
- Degraer, S., Van Lancker, V., Moerkerke, G., Van Hoey, G., Vanstaen, K., Vincx, M. & Henriët, J.-P., 2003. Evaluation of the ecological value of the foreshore: habitat-model and macrobenthic side-scan sonar interpretation: extension along the Belgian Coastal Zone, Report, Ghent University, Belgium.
- Dean R.B., 1974. AERO Report 74-11. Imperial College, London.
- Dodd, N., Blondeaux, P. Calvete, D., De Swart, H., Falques, A., Hulscher, S.J.M.H., Rozynski, G., Vittori, G., 2003. The use of stability methods for understanding the morphodynamical behaviour of coastal systems. *Journal of Coastal Research* 19, 849-865.
- Eckman, J.E., 1983. Hydrodynamic processes affecting benthic recruitment. *Limnology and Oceanography* 28, 241-257.
- Eckman, J.E., Nowell, A.R.M., Jumars, P.A., 1981. Sediment destabilization by animal tubes. *Journal of Marine Research* 39,361-374.
- Fredsoe & Deigaard (Edt.), 1992. *Mechanics of coastal sediment transport*. Advance Series on Ocean Engineering. World Scientific, Singapore, xviii+369 p.
- Gerkema T. 2000. A linear stability analysis of tidally generated sand waves. *Journal of Fluid Mechanics* 417, 303-322.
- Heip, C., Basford, D., Craeymeersch, J.A., Dewarumez, J.-M., Dörjes, J., De Wilde, P., Duineveld, G., Eleftheriou, A., Herman, P.M.J., Niermann, U., Kingston, P., Künitzer, A., Rachor, E., Rumohr, H., Soetaert, K. & Soltwedel, T., 1992. Trends in biomass, density and diversity of North Sea macrofauna. *Journal of Marine Science* 49, 13-22.
- Hulscher, S.J.M.H. 1996. Tidal-induced large-scale regular bed form patterns in a three-dimensional shallow water model. *Journal of Geophysical Research* C9, 101, 20727-20744.
- Hulscher, S.J.M.H. & Van den Brink, G.M. 2001. Comparison between predicted and observed sand waves and sand banks in the North Sea. *Journal of Geophysical Research* C5, 106, 9327-9338.
- Knaapen, M.A.F., Holzhauer, H., Hulscher, S.J.M.H., Baptist, M.J. & van Ledden, M., 2003. On the modeling of biological effects on morphology in estuaries and seas. *Proceedings third IAHR Symposium on River, Coastal and Estuarine Morphodynamics*, 773-783.
- Komarova, N.L. & Hulscher S.J.M.H. 2000. Linear instability mechanism for sand wave formation. *Journal of Fluid Mechanics* 413, 219-246.
- Künitzer, A., Duineveld, G.C.A., Basford, D., Dewarumez, J.-M., Dörjes, J., Eleftheriou, A., Heip, C., Herman, P.M.J., Kingston, P., Niermann, U., Rumohr, H. & De Wilde, P.A.W.J., 1992. The benthic infauna of the North Sea: species distribution and assemblages. *Journal of Marine Science* 49, 127-143.
- Németh, A.A., Hulscher, S.J.M.H. & de Vriend, H.J., 2002. Modelling sand wave migration in shallow shelf seas. *Continental Shelf Research* 22, 2795-2806.
- O'Donoghue, T., Doucette, J.S., van der Werf, J.J. & Ribberink, J.S., 2006. The dimensions of sand ripples in full-scale oscillatory flows. *Coastal Engineering* 53, 997-1012.
- Rabaut, M., Guilini, K., Van Hoey, G., Vincx, M. & Degraer, S., 2007. A bio-engineered soft-bottom environment: The impact of *Lanice conchilega* on the benthic species-specific densities and community structure. *Estuarine, Coastal and Shelf Science* 75, 525-536.
- Sleath, J.F.A., 1984. *Seabed mechanics*. John Wiley & Sons, xv+335 p.
- Soulsby, R.L. & Whitehouse, R.J.S. 2005 Prediction of ripples properties in shelf seas: Mark 2 Predictor for Time Evolution. *Rep. TR 154*, HR Wallingford Ltd, Wallingford UK.
- Van der Veen, H.H., Hulscher, S.J.M.H. & Knaapen, M.A.F. 2006. Grain size dependency in the occurrence of sand waves. *Ocean Dynamics* 56, 228-234.
- Van Hoey, G., Degraer, S. & Vincx, M., 2004. Macrobenthic community structure of soft-bottom sediments at the Belgian Continental Shelf. *Estuarine, Coastal and Shelf Science* 59, 599-613.
- Van Rijn, L.C., 1991. Sediment transport in combined waves and currents, in *Proceedings of Euromech 262*, Balkema, A.A., Brookfield, Vt.